

High Selectivity Differential Bandpass Filter Using Dual-Behavior Resonators

Xin Gao, Wenjie Feng*, and Wenquan Che

Abstract—A high selectivity differential bandpass filter (BPF) using two pairs of dual-behavior resonators (DBRs) is proposed in this letter. A high selectivity passband for the differential mode with second harmonic suppression is achieved, by utilizing shorted coupled lines with two short stubs. For the commonmode (CM) circuit, the CM responses can be suppressed over a wide frequency band by the loaded open/shorted stubs. To validate the feasibility of the proposed filter, a planar differential BPF (3-dB fractional bandwidth 4.9%) with good CM suppression is designed and fabricated. The theoretical and measured results agree well and show good in-band filtering performances and out-of-band harmonic suppression performances.

1. INTRODUCTION

Differential circuits have played an important role in modern wireless communication systems, due to their relatively high immunity to environmental noise, interference and crosstalk between different elements. Among various differential circuits, differential filter as a basic component occupies a pivotal position. Recently, many different differential filters with desired differential-mode (DM) frequency responses and common-mode (CM) suppression have been demonstrated [1–7]. In [1], the double-sided parallel-strip line (DSPSL) dual-mode resonator was adopted to design the narrow differential BPF. However, the upper stopband for the DM operation is a little narrow and CM suppression is not so good. In addition, various coupling structures were used to design differential BPFs, such as coupled lines [2] and coupled resonators [3]. However, the design and analysis of the coupling structures are a little complex. An S-shaped complementary split ring resonator [4] and open complementary split ring resonators [5] were also used to realize good CM suppression in the passband, respectively, but the out-of-band suppression of CM signal is not good. In addition, the wideband differential filters were implemented by T-shaped structure with open/shorted stubs in [6], or stepped-impedance resonators (SIRs) in [7].

The dual-behavior resonator (DBR) has been widely used in single/dual/tri-band filters [8–10] and duplexers [11, 12] with multiple transmission zeros. However, little research has described the application of the DBR in the differential filters. In this work, a novel high selectivity differential bandpass filter using two pairs of DBRs is proposed. Four controllable transmission zeros without complex coupling structures are introduced to suppress spurious resonances of both sides of the bandpass responses for the DM and the upper stopband can be extended to $2.78f_0$. Wideband CM suppression can be also realized by using the all-bandstop transmission characteristic of the coupling circuit. For demonstration, a prototype of the differential bandpass filter operating at 2.45 GHz is constructed on the dielectric substrate Rogers 5880 with $\epsilon_r = 2.2$, $h = 0.508$ mm, and $\tan \delta = 0.0009$.

Received 7 April 2015, Accepted 21 May 2015, Scheduled 22 May 2015

* Corresponding author: Wenjie Feng (fengwenjie1985@163.com).

The authors are with Department of Communication Engineering, Nanjing University of Science & Technology, Nanjing 210094, China.

2. PROPOSED DIFFERENTIAL BPF USING DBRS

Figure 1(a) shows the ideal circuit of the proposed differential BPF which consists of two pairs of DBRs with two open/shorted stubs ($\theta_3, \theta_4, Z_3, Z_4$). The pair of DBRs is composed of two side-coupled shorted lines (θ_1, Z_1 , even/odd-mode characteristic impedance Z_{oe}, Z_{oo}) and two pairs of transmission lines ($\theta_2, \theta_5, Z_2, Z_1$). The four-port filter is ideally symmetric with respect to the central plane in horizon (dotted-line). The equivalent half circuits of the DM/CM can be used for theoretical analysis conveniently [13] as shown in Figures 1(b) and (c).

2.1. Differential/Common Mode Analysis

When the DM signals are excited from Ports 1 and 1' in Figure 1(a), a virtual short appears along the symmetric line, as shown in Figure 1(b). The input admittance Y_{in1} and the external quality factor Q_e of Figure 1(b) can be written as [14]:

$$Y_{in1} = -j \cot(\theta_1 + \theta_5) / Z_1 - j \cot \theta_2 / Z_2 \quad (1)$$

$$Q_e = 0.5 R_L ((\theta_1 + \theta_5) \csc^2(\theta_1 + \theta_5) / Z_1 + \theta_2 \csc^2 \theta_2 / Z_2) \quad (2)$$

And R_L is the load impedance for Z_1 and Z_2 . As discussed in [14], the desired transmission zeros can be easily obtained when $\theta_1 + \theta_5$ equals to π . When $Y_{in1} = 0$, the resonant condition of two shorted stubs can be obtained, and the external quality factor Q_e of the bandpass filter can be selected from the required value of filter specification, then the two unknown variables $\theta_1 + \theta_5$ and θ_2 can be solved when the ratio of Z_1/Z_2 is fixed, in which additional impedance transformer can be avoided [14].

The simulated frequency responses of Figure 1(b) are shown in Figures 2(a)–(b). The bandwidth of DM increases as k increases ($k = (Z_{oe}Z_{oo})/(Z_{oe} + Z_{oo})$). To realize strong coupling of the side-coupled lines for the passband, here we choose $Z_1 > Z_2$. Obviously, two transmission zeros (f_{tz1}, f_{tz2}) are realized by the shorted stub (θ_1, Z_1), and another two transmission zeros (f_{ctz1}, f_{ctz2}) are obtained by the bandstop transmission characteristic of the side-coupled lines. Moreover, the frequencies of f_{tz1}, f_{tz2} decrease as the electrical length (θ_1) of shorted stubs increases when the ratio of Z_1/Z_2 is fixed. Meanwhile Q_e increases as θ_1 increases. In addition, θ_5 has a great influence on the out-of-band suppression. Due to the electrical length of the side-coupled lines is still θ_1 , the two transmission zeros (f_{ctz1}, f_{ctz2}) do not change.

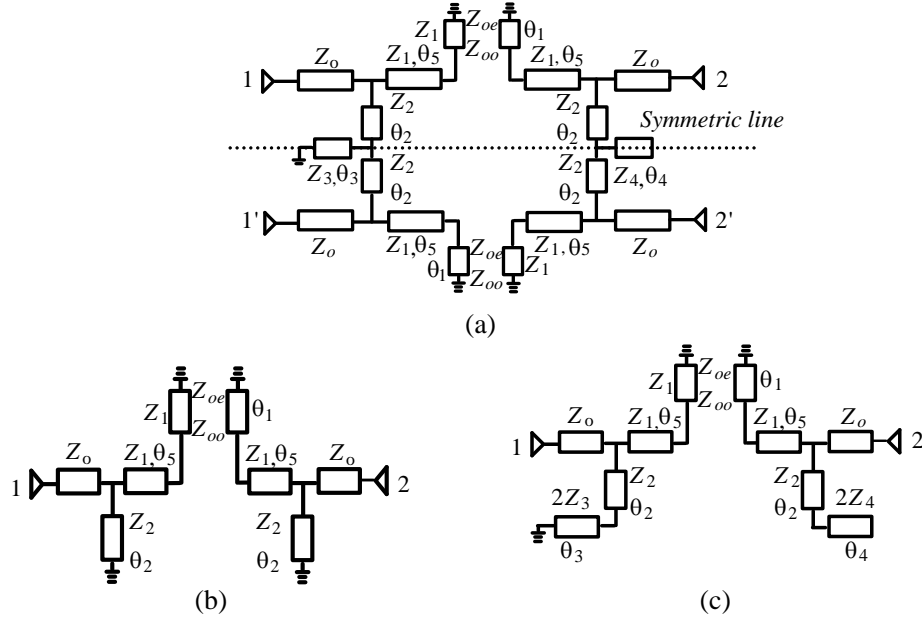


Figure 1. (a) Ideal circuit of the differential filter using DBRs, (b) equivalent circuit for the differential mode, (c) equivalent circuit for the common mode.

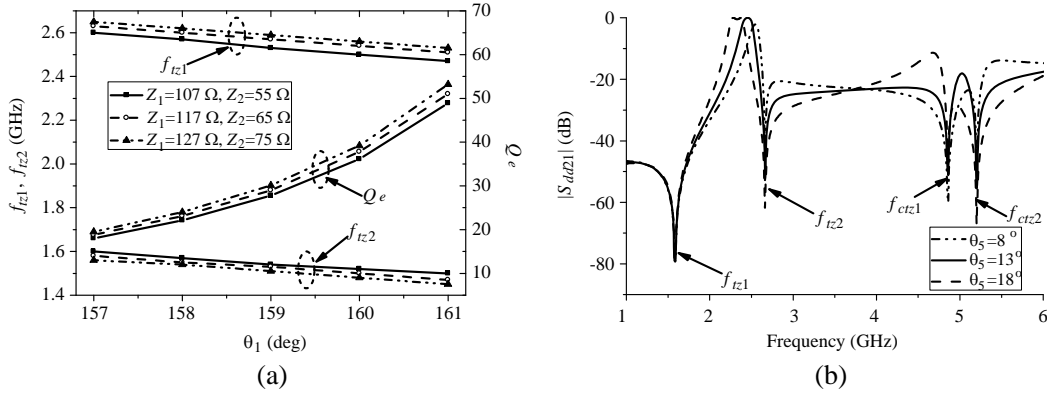


Figure 2. Simulated frequency responses of the differential mode of Figure 1(b), (a) versus θ_1 , $\theta_5 = 13^\circ$, (b) versus θ_5 , $\theta_1 = 159^\circ$, $\theta_2 = 13^\circ$, $Z_1 = 117 \Omega$, $Z_{oe} = 147.6 \Omega$, $Z_{oo} = 75.8 \Omega$, $Z_2 = 65 \Omega$, ($Z_o = 50 \Omega$, $f = 2.45$ GHz).

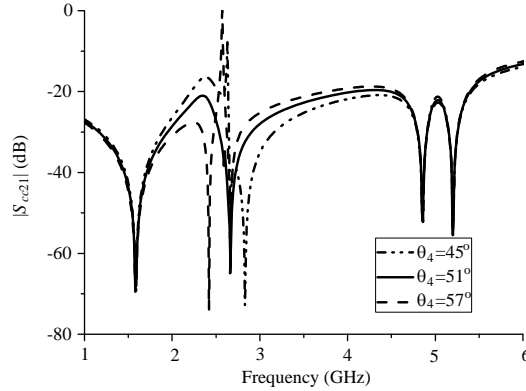


Figure 3. Simulated frequency responses of the common mode of Figure 1(c) versus θ_4 , $\theta_1 = 159^\circ$, $\theta_2 = 13^\circ$, $\theta_5 = 13^\circ$, $Z_o = 50 \Omega$, $Z_1 = 117 \Omega$, $Z_2 = 65 \Omega$, $f = 2.45$ GHz.

When the CM signals are excited from Ports 1 and 1' in Figure 1(a), a virtual open appears along the symmetric line, as shown in Figure 1(c). According to the preceding description, the CM operation circuit is based on the allstop transmission characteristic of the side-coupled lines with open loaded stubs. However, the open stub (θ_2 , Z_2) causes a harmonic response. To eliminate the impact, two open/shorted stubs (θ_3 , θ_4 , Z_3 , Z_4) are introduced to suppress the response. For the common mode, the input impedance Z_{in2} can be written as:

$$Y_{in2} = -j \cot(\theta_1 + \theta_5)/Z_1 + j \frac{Z_2 + 2Z_4 \cot \theta_4 \tan \theta_2}{2Z_2 Z_4 \cot \theta_4 - Z_2^2 \tan \theta_2} \quad (3)$$

When $Z_{in2} = 1/Y_{in2} = 0$, the transmission zero occurs at the center frequency. As we can see, good CM suppression in a wide band can be obtained by properly choosing θ_4 , as shown in Figure 3. Meanwhile, the shorted stub (θ_3 , Z_3) only has a little effect on the harmonic suppression. In this way, a differential filter with high selectivity and wideband CM suppression can be easily realized.

2.2. Proposed Differential Bandpass Filter

To demonstrate the proposed concepts, an experimental Chebyshev bandpass filter is implemented with fraction bandwidths of 4.9%. Based on the required responses, the lumped element values of the second-order prototype filter are determined as follows: $g_0 = 1$, $g_1 = 1.4029$, $g_2 = 0.7071$, $g_3 = 1.9841$. The required coupling coefficient and the external quality factor can be obtained based on [15]

$$Q_e = g_0 g_1 / FBW, \quad k = FBW / \sqrt{(g_1 g_2)} \quad (4)$$

It can be calculated that $Q_e = 28.6$ and $k = 0.049$. The Q_e factor and the coupling coefficient are extracted based on [15]

$$Q_e = f_0 / \Delta f_{\pm 90^\circ}, \quad k = (f_2^2 - f_1^2) / (f_2^2 + f_1^2) \quad (5)$$

where f is the resonant frequency and $\Delta f_{\pm 90^\circ}$ the bandwidth over which the phase shifts $\pm 90^\circ$ with respect to the absolute phase at f_0 , and f_1 and f_2 are the two resonant frequencies of the shorted coupled lines. First of all, choose the desired center frequency f_0 of the differential mode, and according to (1)–(2), choose the proper Q_e and ratio of Z_1/Z_2 to obtain the desired $\theta_1 + \theta_5$ and θ_2 . And then adjust coupling gap (g) and θ_1 to realize better transmission characteristic for the differential mode. Finally, optimize the two open/shorted stubs ($\theta_3, \theta_4, Z_3, Z_4$) to maximize the common mode suppression. Based on the above theoretical analysis, the final parameters for the proposed differential BPF circuit of Figure 1(a) are given below: $Z_0 = 50 \Omega$, $Z_1 = 117 \Omega$, $Z_2 = 65 \Omega$, $Z_3 = 30 \Omega$, $Z_4 = 19 \Omega$, $Z_{oe} = 141 \Omega$, $Z_{oo} = 84 \Omega$, $\theta_1 = 162^\circ$, $\theta_2 = 14^\circ$, $\theta_3 = 40^\circ$, $\theta_4 = 56^\circ$, $\theta_5 = 15^\circ$, $f_0 = 2.45$ GHz. Figure 4 shows the top view and photograph of the proposed differential BPF. The simulated results are shown in Figure 5 (Ansoft HFSS v.13). For the DM, a second-order passband with 3-dB bandwidth 5.2% (2.35–2.48 GHz) is realized. The insertion loss ($|S_{dd21}|$) is less than 0.7 dB while the return loss ($|S_{dd11}|$) is over 18 dB at f_0 . Four transmission zeros are found to locate at 1.62 GHz, 2.67 GHz, 4.78 GHz and 5.18 GHz. Furthermore, over 18-dB upper stopband is obtained (2.54–6.14 GHz, $2.5f_0$). For the CM, the insertion loss ($|S_{cc21}|$) is greater than 15 dB (0–5.5 GHz, $2.25f_0$).

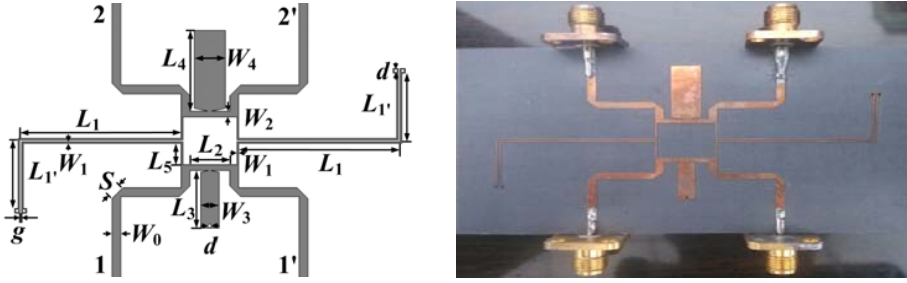


Figure 4. Top view and photograph of the differential BPF ($L_1 = 28$ mm, $L_{1'} = 11.9$ mm, $L_2 = 6.8$ mm, $L_3 = 10$ mm, $L_4 = 14$ mm, $L_5 = 3.7$ mm, $W_0 = 1.53$ mm, $W_1 = 0.3$ mm, $W_2 = 1$ mm, $W_3 = 3.1$ mm, $W_4 = 5.3$ mm, $d = 0.6$ mm, $g = 0.3$ mm, $S = 2.63$ mm, 34 mm \times 67 mm).

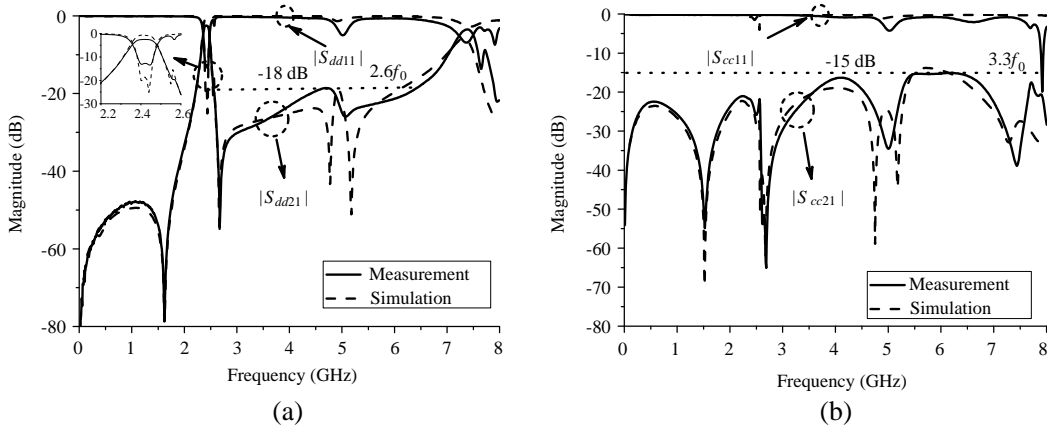


Figure 5. Measured and simulated results for the proposed differential BPF, (a) differential mode, (b) common mode.

Table 1. Comparisons of measured results for some differential filters.

Filter Structures	Transmission zeros, $ S_{dd21} $ 0- $2f_0$ (f_0)	3-dB bandwidth $ S_{dd21} $	Upper stopband $ S_{dd21} $, dB	$ S_{cc21} $, dB (GHz)
Ref. [1]	2 (2.5 GHz)	12%	< -15 ($1.6f_0$)	< -15 (1.5-4)
Ref. [2]	2 (2.0 GHz)	10.5%	< -15 ($3.0f_0$)	< -15 (0-5.8)
Ref. [2]	2 (2.05 GHz)	97%	< -15 ($3.2f_0$)	< -15 (0-5.2)
Ref. [4]	1 (1.0 GHz)	10%	< -15 ($1.8f_0$)	< -15 (0-1.2)
Ref. [7]	1 (2.4 GHz)	40%	< -15 ($2.1f_0$)	< -15 (1.4-3)
This work	3 (2.45 GHz)	4.9%	< -15 ($2.6f_0$)	< -15 (0-8)

3. MEASURED RESULTS AND DISCUSSION

Figure 5 shows the measured results of the proposed differential BPF. For the performances of DM in Figure 5(a), three transmission zeros are located at 1.62 GHz, 2.67 GHz and 5.06 GHz (3-dB bandwidth 4.9%, 2.36–2.48 GHz) respectively. The measured insertion loss is less than 2.4 dB while the return loss is over 13 dB in the passband. Furthermore, over 18-dB upper stopband is achieved from 2.54 to 6.45 GHz ($2.6f_0$). For the performances of CM, as shown in Figure 5(b), over 15-dB stopband is obtained from 0 to 8.0 GHz ($3.3f_0$). The slight frequency discrepancies between the measured and simulated results are mainly caused by the limited fabrication precision and measurement errors.

For the purpose of comparison, Table 1 illustrates the measured results for some differential structures. Obviously, compared with former works, the upper stopbands for the differential mode and the stopbands for the common mode suppression of the proposed filter show better performances.

4. CONCLUSION

In this letter, a novel high selectivity differential BPF based on DBRs is proposed. The out-of-band suppression of DM and CM operation can be easily obtained by the bandstop transmission characteristic of the side-coupled coupled lines. Compared with former differential structures, the proposed differential filter has simpler circuit structures and wider common mode suppression. Good agreements between simulated and measured responses of the filter are demonstrated, indicating a good candidate for wireless applications.

ACKNOWLEDGMENT

This work is supported by the National Natural Science Foundation of China (6140010914), the 2012 Distinguished Young Scientist awarded by the National Natural Science Foundation Committee of China (61225001), Natural Science Foundation of Jiangsu Province (BK20140791) and the 2014 Zijin Intelligent Program of Nanjing University of Science and Technology.

REFERENCES

1. Shi, J., J.-X. Chen, and Q. Xue, "A novel differential bandpass filter based on double-sided parallel-strip line dual-mode resonator," *Microw. Opt. Technol. Lett.*, Vol. 5, 1733–1735, 2008.
2. Wu, C.-H., C.-H. Wang, and C. H. Chen, "Novel balanced coupled-line bandpass filters with common-mode noise suppression," *IEEE Trans. Microw. Theory Tech.*, Vol. 55, 287–295, 2007.
3. Wu, C.-H., C.-H. Wang, and C. H. Chen, "Balanced coupled resonator bandpass filters using multisection resonators for common-mode suppression and stopband extension," *IEEE Trans. Microw. Theory Tech.*, Vol. 55, 1756–1763, 2007.

4. Horestani, A. K., M. Durán-Sindreu, J. Naqui, C. Fumeaux, and F. Martín, “S-shaped complementary split ring resonators and their application to compact differential bandpass filters with common-mode suppression,” *IEEE Microw. Wireless Compon. Lett.*, Vol. 24, 149–151, 2014.
5. Vélez, P., J. Naqui, A. Fernández-Prieto, M. Durán-Sindreu, J. Bonache, J. Martel, F. Medina, and F. Martín, “Differential bandpass filter with common-mode suppression based on open split ring resonators and open complementary split ring resonators,” *IEEE Microw. Wireless Compon. Lett.*, Vol. 23, 22–24, 2013.
6. Feng, W. J. and W. Q. Che, “Novel wideband differential bandpass filters based on T-shaped structure,” *IEEE Trans. Microw. Theory Tech.*, Vol. 60, 1560–1568, 2012.
7. Vélez, P., M. Durán-Sindreu, J. Bonache, A. F. Prieto, J. Martel, F. Medina, and F. Martín, “Differential bandpass filters with common-mode suppression based on stepped impedance resonators (SIRs),” *Proc. IEEE MTT-S Int. Microw. Symp.*, 1–4, Seattle, WA, USA, Jun. 2013.
8. Su, T., S.-J. Wang, Y.-L. Zhang, and Z.-P. Li, “A compact DBR filter using π -network and dual-line equivalent circuit,” *IEEE Microw. Wireless Compon. Lett.*, Vol. 23, 350–352, 2013.
9. Hua, C.-Z., C. Miao, and W. Wu, “A novel dual-band bandpass filter based on DBR,” *Asia Pacific Microwave Conference*, 1383–1386, 2009.
10. Quendo, C., E. Rius, A. Manchec, Y. Clavet, B. Potelon, J.-F. Favennec, and C. Person, “Planar tri-band filter based on dual behavior resonator,” *Proc. Eur. Microw. Conf.*, 269–272, Oct. 2005.
11. Srisathit, K., R. Phromlounsri, S. Patisang, and M. Chongcheawchamnan, “A new microstrip duplexer using open circuited dual-behavior resonator,” *Proc. Asia-Pacific Microw. Conf.*, Dec. 4–7, 2005.
12. Manchec, A., et al., “Ku-band microstrip diplexer based on dual behavior resonator filter,” *IEEE MTT-S Int. Dig.*, 525–528, Long Beach, CA, Jun. 2005.
13. Eisenstant, W. R., B. Stengel, and B. M. Thompson, *Microwave Differential Circuit Design using Mixed-mode-parameters*, Artech House, Boston, MA, 2006.
14. Deng, P. H. and J.-T. Tsai, “Design of microstrip cross-coupled bandpass filter with multiple independent designable transmission zeros using branch-line resonators,” *IEEE Microw. Wireless Compon. Lett.*, Vol. 23, 249–251, 2013.
15. Hong, J. S. and M. J. Lancaster, *Microstrip Filters for RF/Microwave Applications*, Wiley, New York, USA, 2001.